WIKIPEDIA
The Free Encyclopedia

Google Scholar

In mathematics, physics, and art, moiré patterns are large-scale interference patterns… For the moiré interference pattern to appear, the two patterns must not be completely identical, but rather displaced, rotated, or have slightly different pitch.

Twistronics (from twist and electronics) is the study of how the angle (the twist) between layers of two-dimensional materials can change their electrical properties.

twistronics + moiré → over 20,000 papers

Morning: Moiré superlattices in graphene	Afternoon: Twistronics of transition metal dichalcogenides

2D materials family

strongly covalent-bonded atomically thin planes extracted from layered crystals with much weaker van der Waals adhesion between the layers

chemically stable
mechanically robust
bendable
&
stretchable

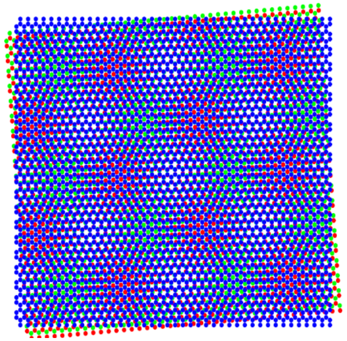

Graphene	hBN 'white graphene'	BCN	Fluorographene	Graphene oxide
Transition metal dichalcogenides (TMD) MoS_2, WS_2, $MoSe_2$, WSe_2	Semiconducting dichalcogenides: $MoTe_2$, WTe_2, ZrS_2, $ZrSe_2$ and so on	Metallic dichalcogenides: $NbSe_2$, NbS_2, TaS_2, TiS_2, $NiSe_2$ and so on superconductors at low temperatures		
		Layered semiconductors: GaSe, GaTe, InSe, Bi_2Se_3 and so on		
Micas, BSCCO	MoO_3, WO_3	Perovskite-type: $LaNb_2O_7$, $(Ca,Sr)_2Nb_3O_{10}$,	Magnetic $CrCl_3$, CrI_3, $CrBr_3$ $RuCl_3$,	

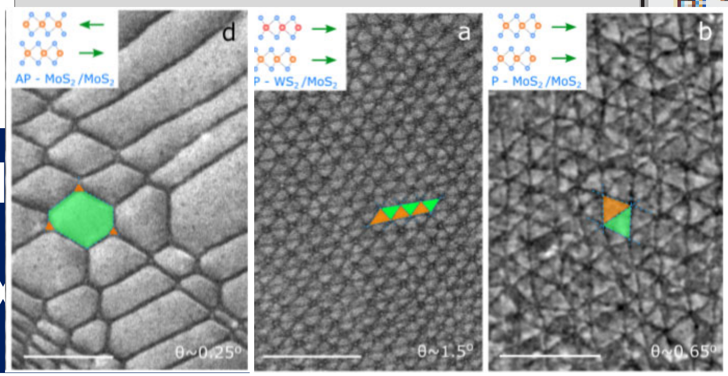

collectively, the alread

which can be further ex

Twistronics of transition metal dichalcogenides

- Structure of twisted bilayers – reconstruction into domains and domain wall networks
- Bilayer with inversion symmetry (AP) and without it (P)
- Ferroelectric interfaces and layer-asymmetric band edges in TMDs
- Switching FE polarisation by sliding and ‘string theory’ for domain wall networks
- Band-edge profiles, arrays of QDs, and ‘narrow moiré minibands’
- Ferroelectric few-layer graphene

Moiré superstructures in TMD bilayers

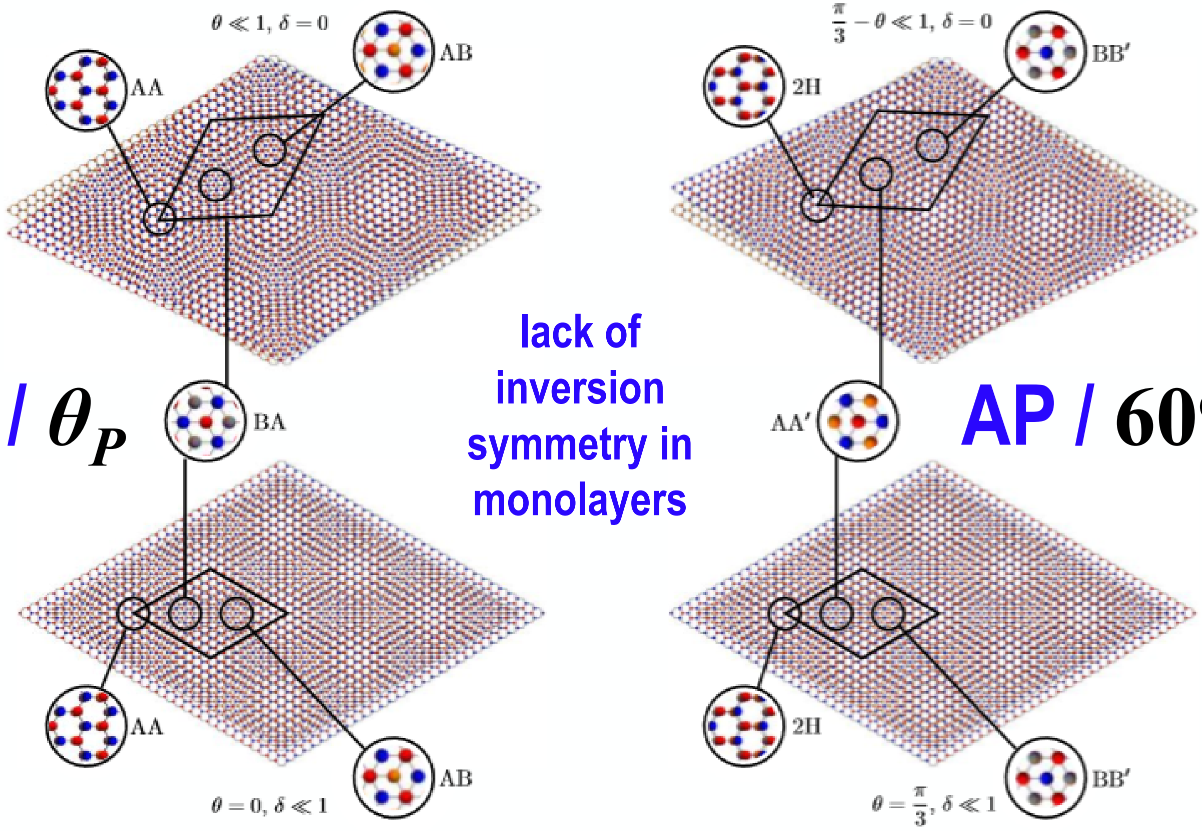

P / θ_P

lack of inversion symmetry in monolayers

AP / $60^o + \theta_{AP}$

are sensitive to P/AP orientation of unit cells in each layer, due to their inversion asymmetry

$MX_2/M'X'_2$ adhesion energy: *ab initio* DFT input

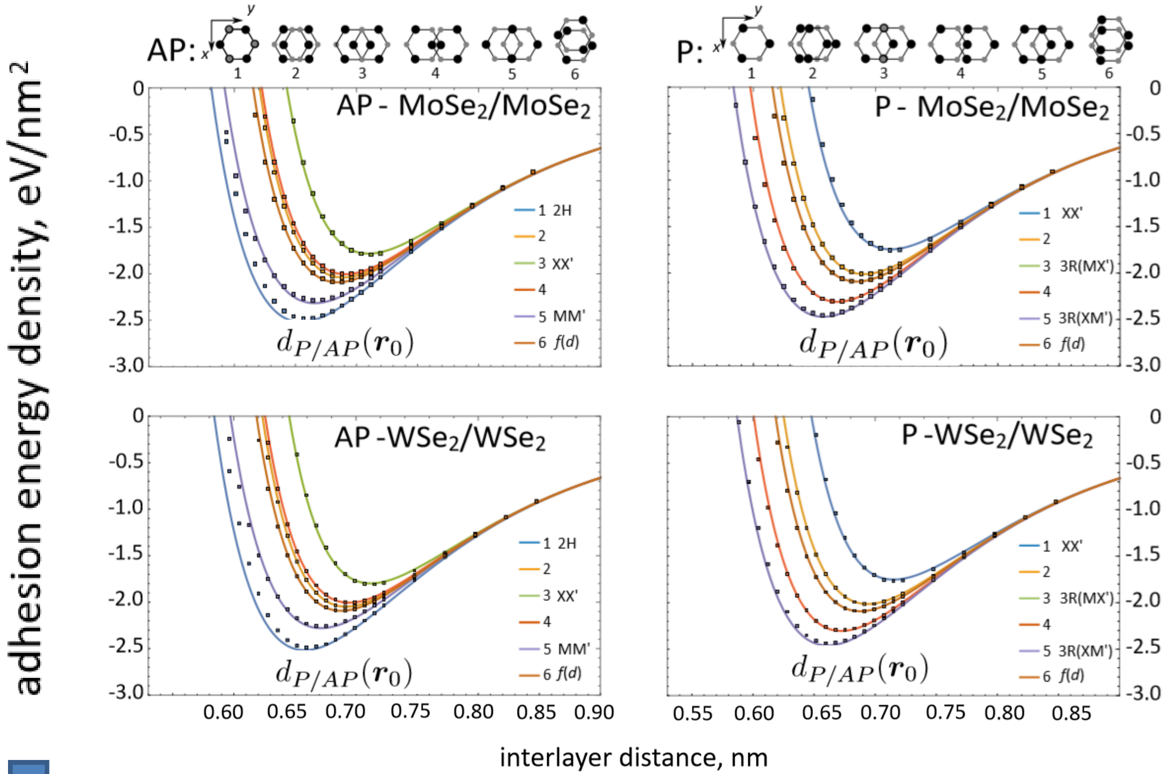

DFT-parametrised for all MX_2 homo- & heterobilayers

M = Mo, W
X = S, Se

sets optimal interlayer distance for each offset $\boldsymbol{r_0}$ between top/bottom layer lattices

$$W_{P/AP}(\boldsymbol{r}_0, d) = -\sum_{n=1}^{3} \frac{C_{4n}}{d^{4n}} + \sum_{n=1}^{3} \left[A_1 e^{-\sqrt{G^2+\rho^{-2}}d} \cos(\boldsymbol{G}_n \boldsymbol{r}_0) + A_2 e^{-Gd} \sin\left(\boldsymbol{G}_n \boldsymbol{r}_0 + \varphi_{P/AP}\right) \right]$$

PRL 124, 206101 (2020)

Mesoscale lattice relaxation (modelling)

minimise elastic + adhesion energy

$$\sum_{l=t,b}\left[(\lambda_l/2)\left(u_{ii}^{(l)}\right)^2+\mu_l\left(u_{ij}^{(l)}\right)^2\right]+W_{P/AP}(\boldsymbol{r}_0,d)$$

$$d_{P/AP}(\boldsymbol{r}_0)$$

$$\boldsymbol{r}_0\left(\boldsymbol{r}\right)=\theta\hat{z}\times\boldsymbol{r}+\delta\boldsymbol{r}+\boldsymbol{u}^{(t)}-\boldsymbol{u}^{(b)}$$

for all MX_2 bilayers
M = Mo, W; X = S, Se

δ – lattice mismatch

θ – misalignment angle

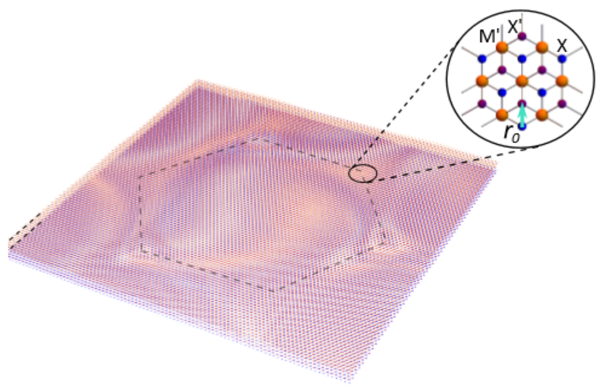

Short-period and long-period moiré structures

large angle or different chalcogens: almost rigid short-period superlattice

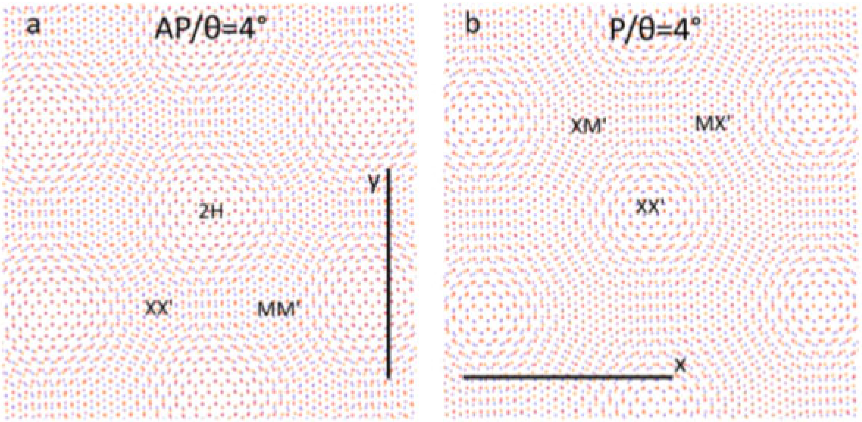

$$\ell \approx a/\sqrt{\theta^2_{P,AP} + \delta^2}$$

$$\theta^*_{AP} \approx 1.0^\circ$$

$$\theta^*_{P} \approx 2.5^\circ$$

small angle same-chalcogen bilayers: domains separated by dislocations

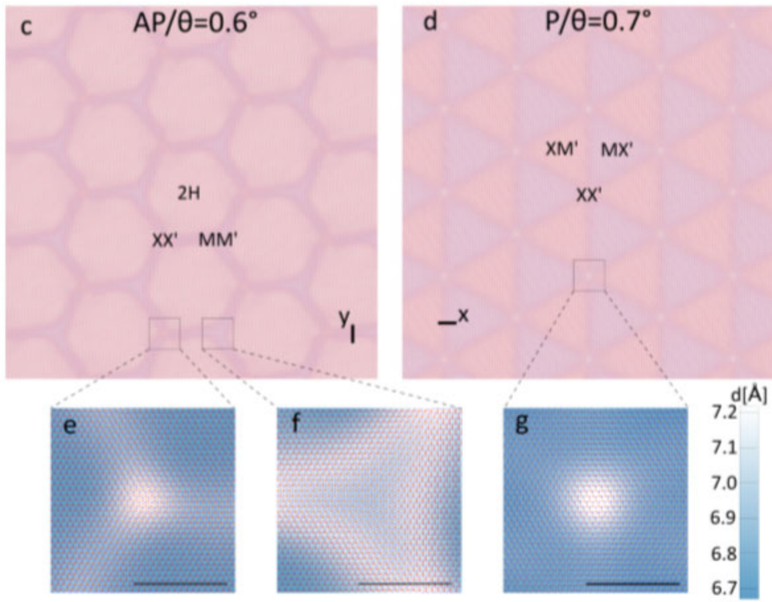

twisted homobilayers: strain is almost pure shear deformations in both layers

same-chalcogen heterobilayers with δ<1%: shear and hydrostatic strain (biaxial) components in each layer

PRL 124, 206101 (2020)

Domains and domain wall networks: STEM

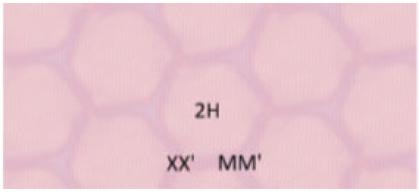

Nature Nanotechnology 15, 592 (May 2020)

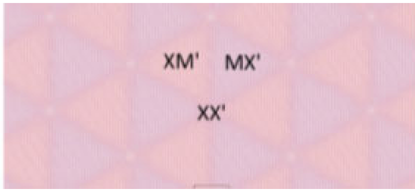

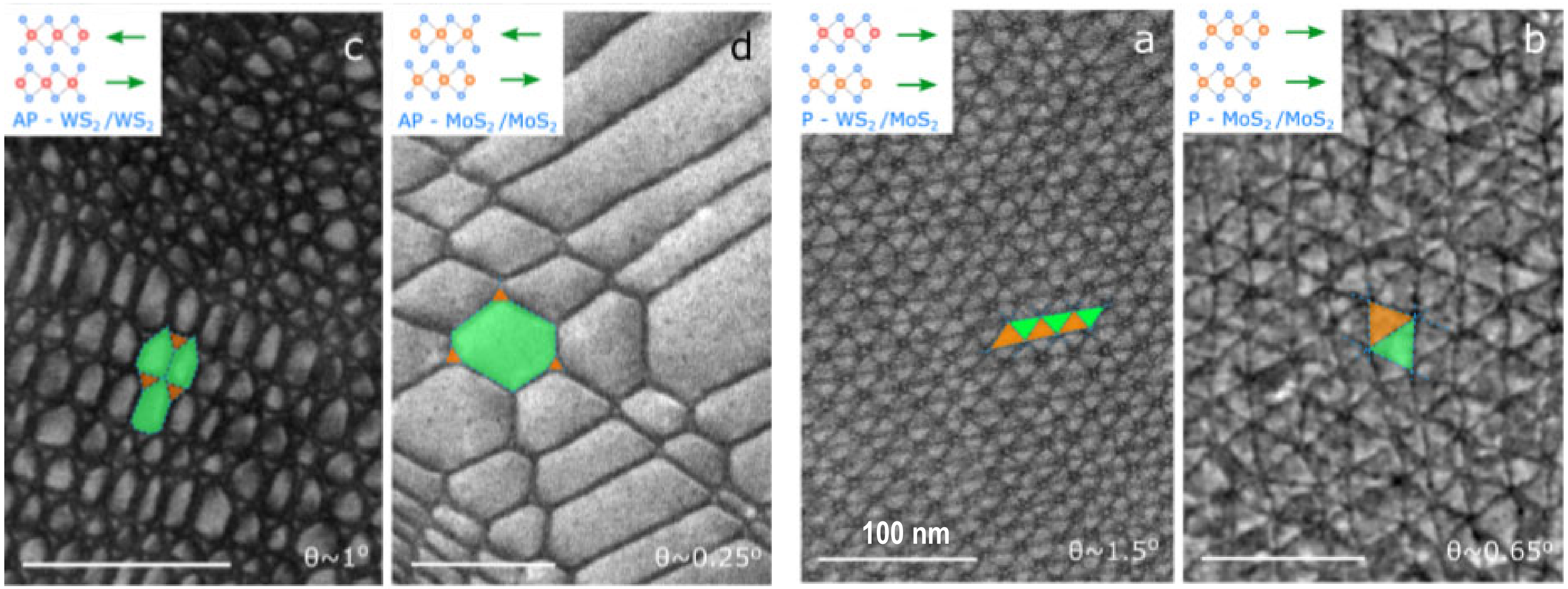

AP-bilayers

Networks of perfect screw dislocations

Piezoelectric domain wall (DW) networks in AP-MX_2 homobilayers

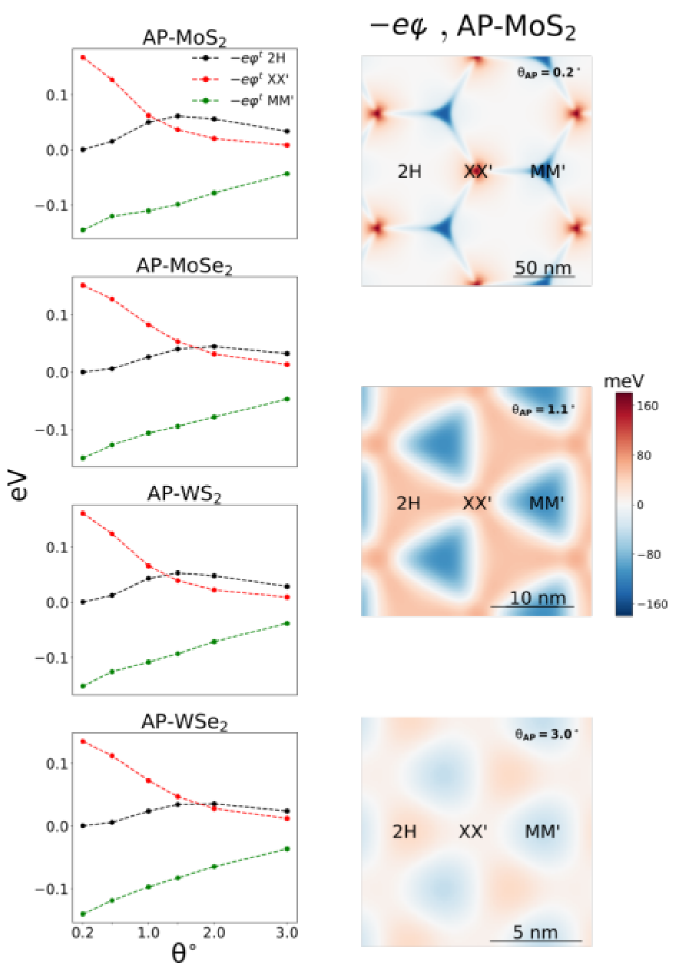

Appl Phys Lett 118, 241602 (2021)

same sign of piezocharges in top & bottom layers

$$\rho = e_{11}\left[2\partial_x u_{xy} + \partial_y(u_{xx} - u_{yy})\right]$$

$$e^t_{11} = -e^b_{11} \qquad u^t_{ij} = -u^b_{ij}$$

Conducting atomic force microscopy (cAFM) and scanning Kelvin probe microscopy (SKPM) revealed piezoelectric charge modulation near DW networks

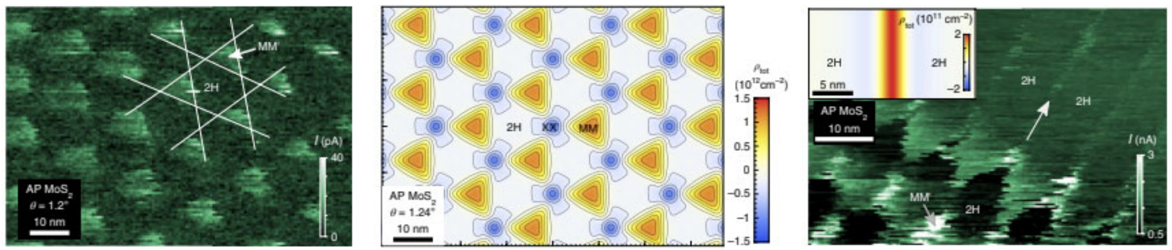

Nature Nano 15, 750 (2020)

Twistronics of transition metal dichalcogenides

- Structure of twisted bilayers – reconstruction into domains and domain wall networks
- Bilayer with inversion symmetry (AP) and without it (P)
- Ferroelectric interfaces and layer-asymmetric band edges in TMDs
- Switching FE polarisation by sliding and ‘string theory’ for domain wall networks
- Band-edge profiles, arrays of QDs, and ‘narrow moiré minibands’
- Ferroelectric few-layer graphene

Domains and domain wall networks: P-bilayers

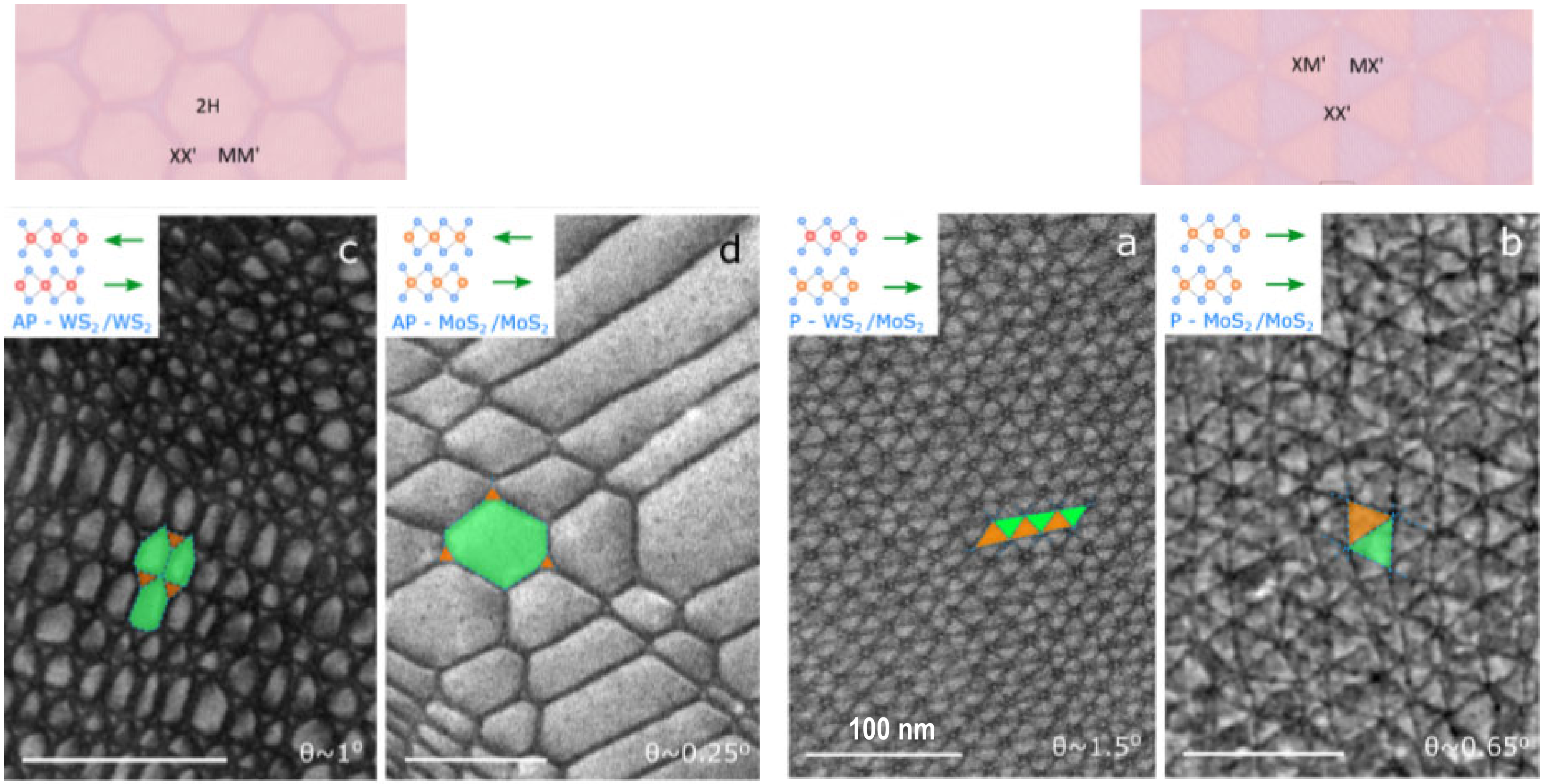

Networks of partial screw dislocations

Weak ferroelectricity in P-homobilayers of TMDs (‘R-stacking’)

spontaneous vertical polarisation due to the interlayer hybridisation of chalcogen orbitals in homobilayers with a broken-symmetry interface (MX and XM) **reversible by sliding**

	$\Delta^P(\mathrm{MX}')$ (meV)
MoS_2	69
$MoSe_2$	67
WS_2	63
WSe_2	66(61)

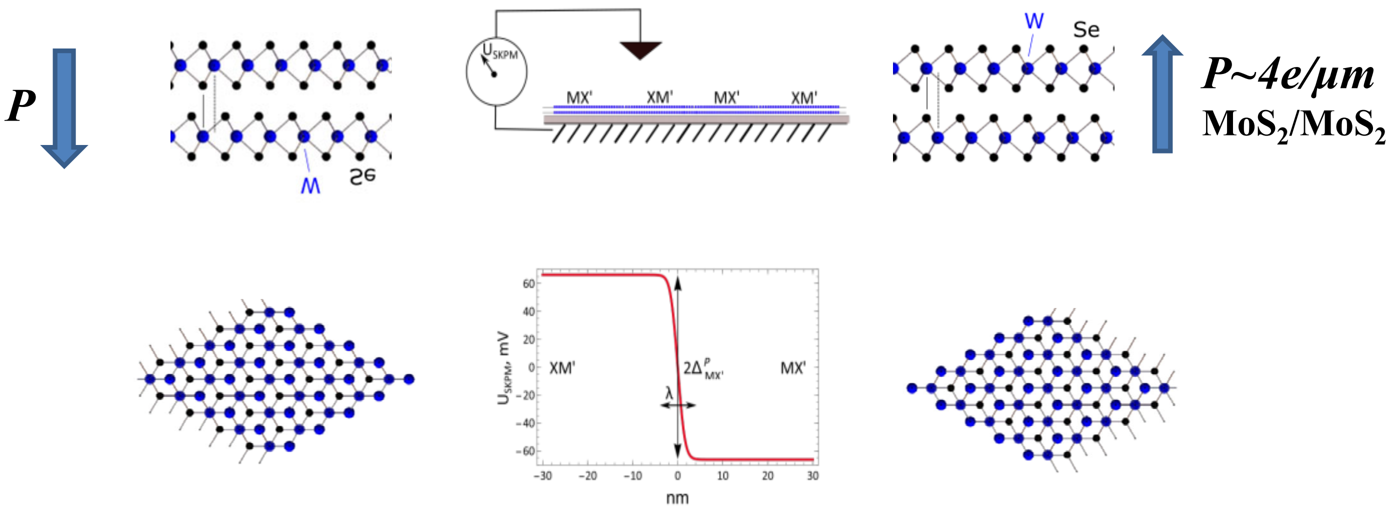

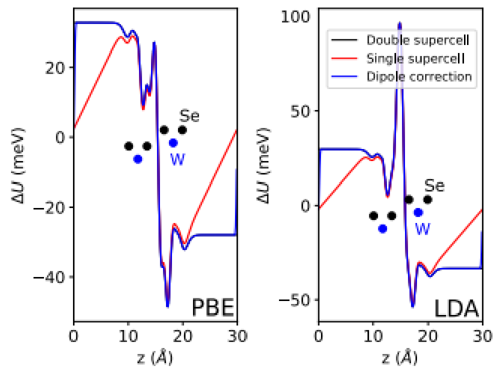

twin structures which can be converted into each other by sliding

Scientific Reports 11, 13422 (2021)

Additive weak ferroelectricity in combinatorial P-homobilayers of TMDs and hBN

$$U - U_0 = -\frac{PD}{\epsilon_0} - \frac{1}{2}\frac{\alpha_{zz}^{2L} D^2}{\epsilon_0 \mathcal{A}}$$

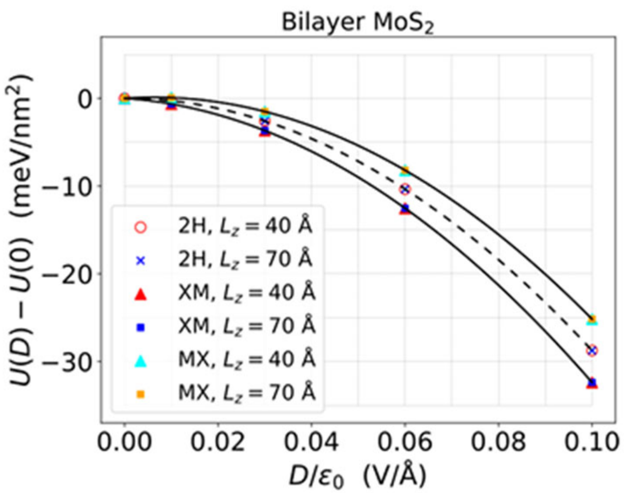

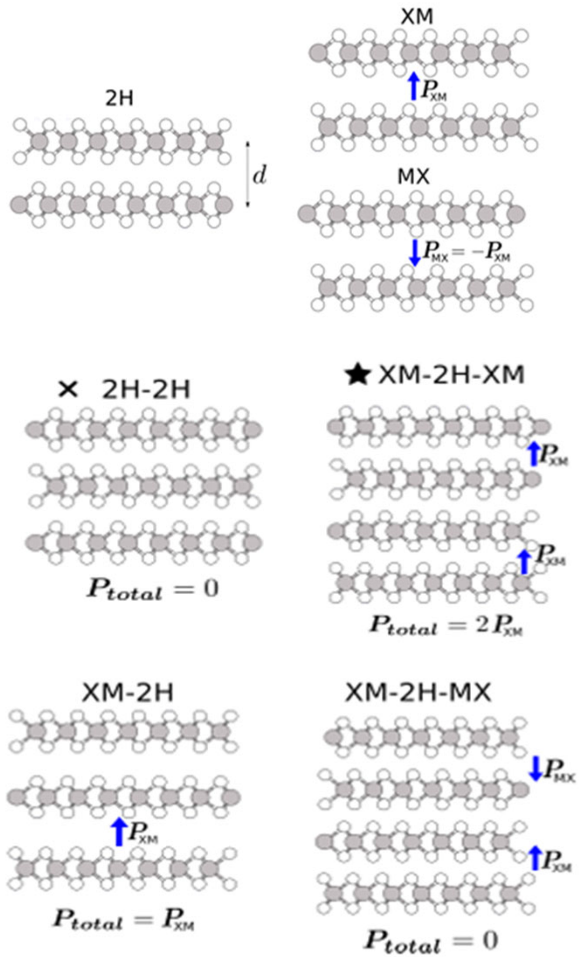

	hBN	FP interfaces	P ($10^{-4} e/\text{Å}$)
1L			0
2L	BN^{AP}		0
	BN^{P}	P_{BN}	5.5
	NB^{P}	P_{NB}	−5.4
3L	BN^{AP}-BN^{AP}		0
	BN^{P}-NB^{P}	$P_{BN} + P_{NB}$	0
	BN^{P}-BN^{P}	$2P_{BN}$	11.7
4L	BN^{AP}-BN^{AP}-BN^{AP}		0
	BN^{P}-NB^{P}-BN^{P}	$2P_{BN} + P_{NB}$	6.3
	BN^{P}-BN^{P}-BN^{P}	$3P_{BN}$	17.9

Phys Rev B 106, 125408 (2022)

Kelvin microscopy of ferroelectric domains in marginally twisted MoS_2

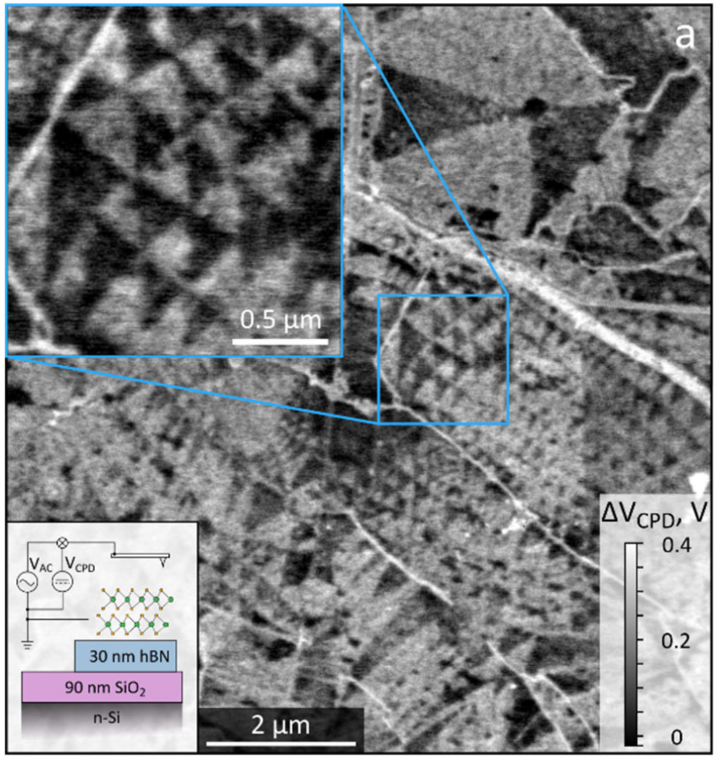

Nature Nano 17, 390 (2022)

Polarization → *potential drop* ΔV^{FE}

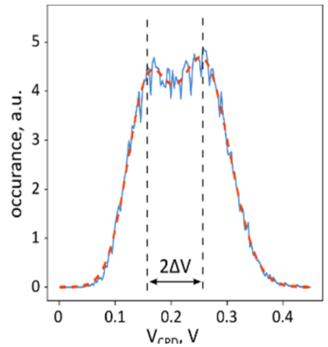

SKPM of MoS_2 bilayers gives Δ=60 meV

	ΔV^{FE}[mV]
MoS_2	69
$MoSe_2$	67
WS_2	63
WSe_2	66(61)

Scientific Reports 11, 13422 (2021)

Electrically tuneable domain structure

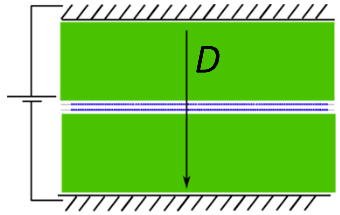

makes XM and MX energetically inequivalent in electric field

$$\mathcal{E} = \sum_{a=t,b} \left[\lambda (u_{ii}^{a})^2 + \mu u_{ij}^{a} u_{ji}^{a}\right] + W(\vec{r}_0, d) - DP(\vec{r}_0, d) \to \vec{u}^{t/b}$$

DW = Partial dislocation (PD)

perfect (full) screw dislocation (PSD) appear

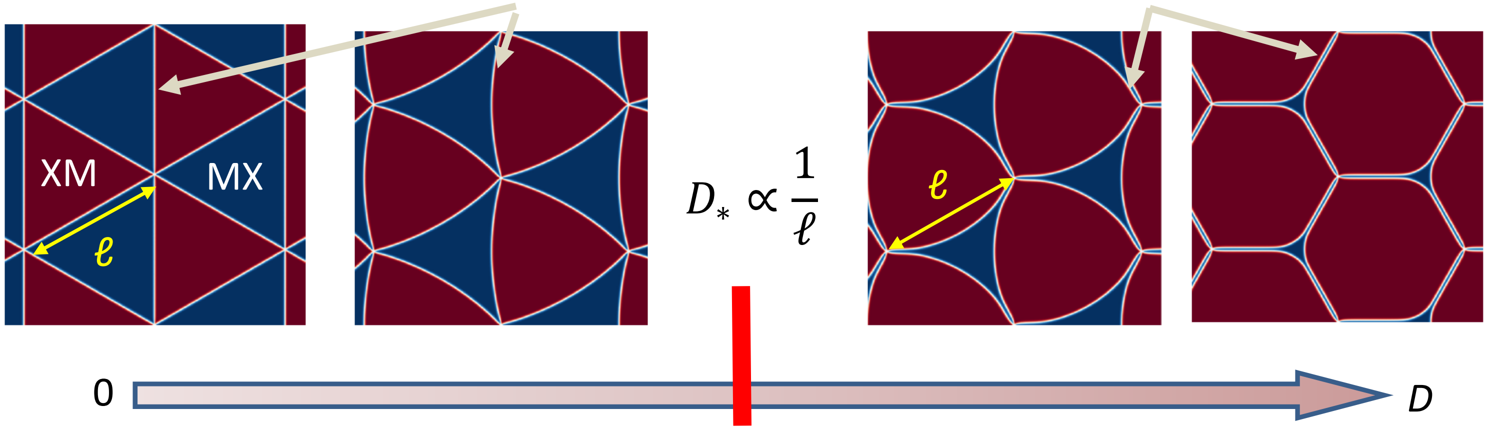

$$D_* \propto \frac{1}{\ell}$$

Electrically tuneable domains in MoS_2/MoS_2

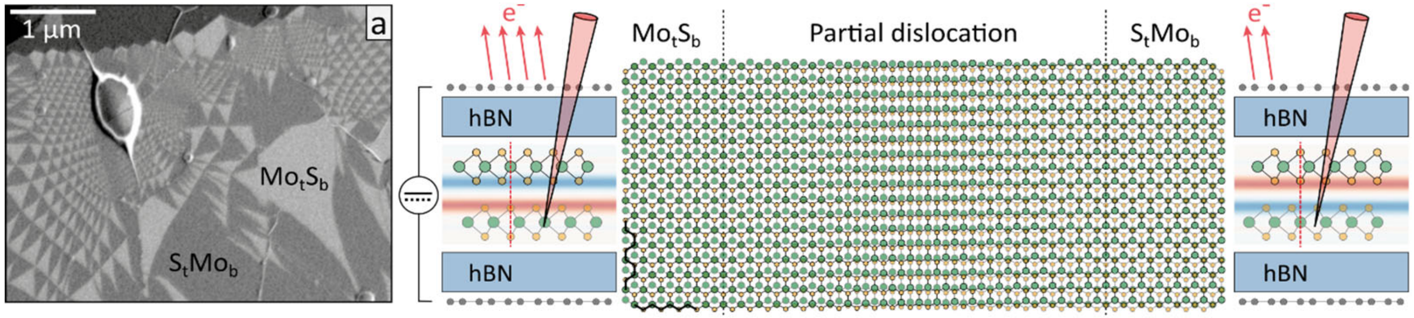

back-scattered electron channelling contrast imaging

polarisation is reversed by interlayer sliding near domain boundaries, detected by SEM imaging

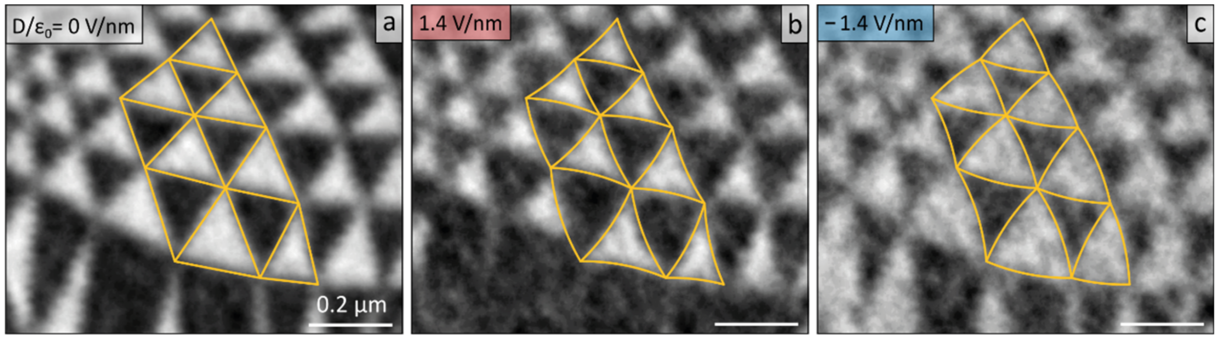

Nature Nanotechnology 17, 390 (2022)

‘string theory’ of tuneable domain wall networks

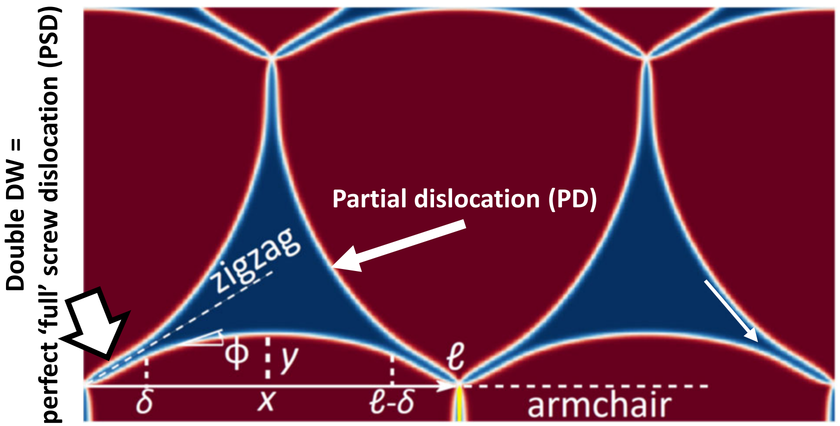

MoS_2

$\overline{w} = 0.94$ eV/nm
$\widetilde{w} = 0.62$ eV/nm

PSD||zigzag
$u = 2.19$ eV/nm

$\frac{2}{\sqrt{3}}\delta$ = length of PSD

PD energy vs. orientation

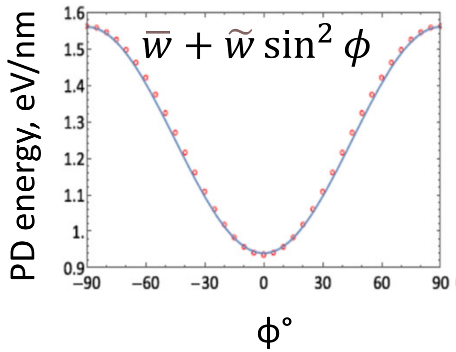

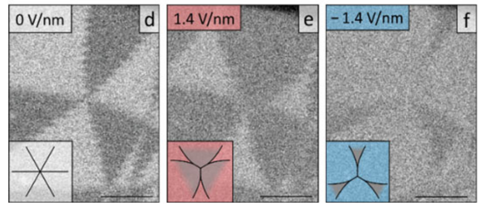

$$\mathcal{E}_\ell[y(x),\delta] = 3\int_{\delta}^{\ell-\delta}\left[\left(\overline{w} + \widetilde{w}\frac{y'^2}{1+y'^2}\right)\sqrt{1+y'^2} - 2\frac{\Delta V^{FE} D}{\chi}y\right]dx + 3\left[u\frac{2\delta}{\sqrt{3}} - 2\frac{\Delta V^{FE} D}{\chi\sqrt{3}}\delta^2\right]$$

PD energy | PD length extension | expansion of favorable domains | PSD energy | expansion of favorable domains

universal solution

$$D_* = \frac{\chi\left(\frac{\overline{w}}{2} + \frac{7\widetilde{w}}{8}\right)}{\Delta V^{FE}\ell}$$

threshold displacement field

Nano Letters 22, 1534 (2022)

Moiré pattern as a magnifying glass for small intra-layer deformations (traced by following XX stacking nodes)

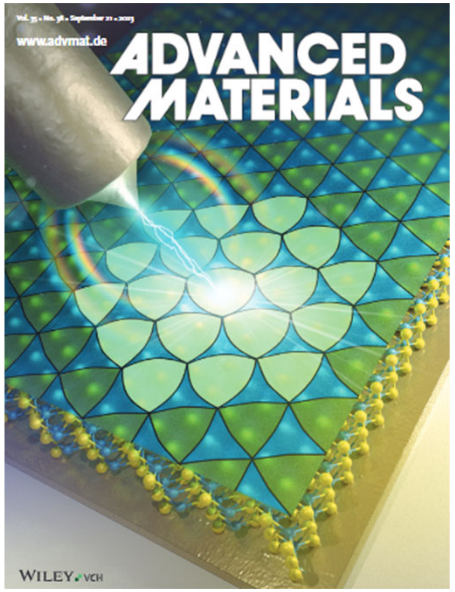

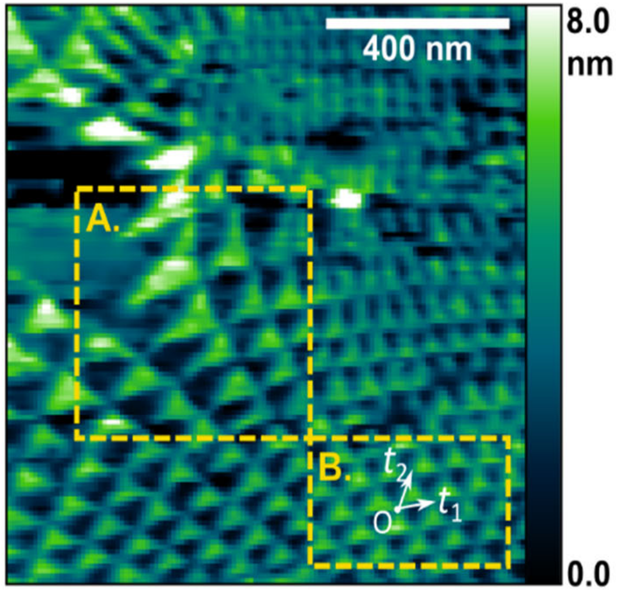

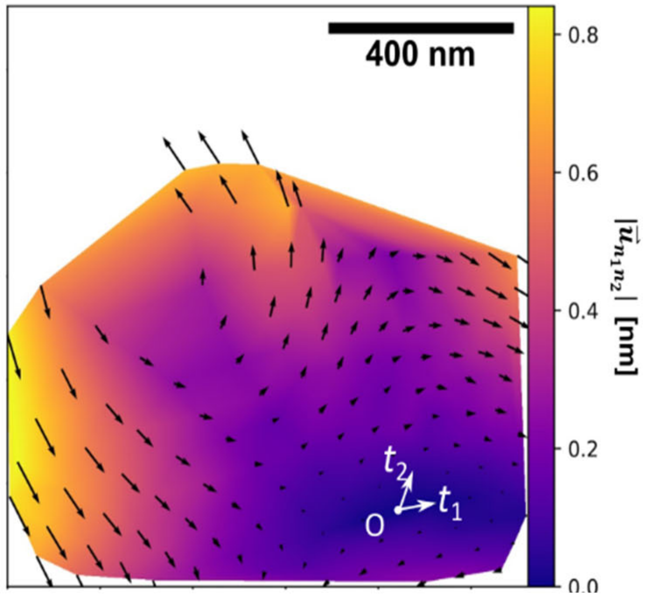

STM mapping of a twisted WS_2 P-bilayer

$$\vec{u}(\vec{R}_{n_1,n_2}) = \theta\hat{z} \times \vec{R}_{n_1,n_2} - n_1\vec{a}_1 - n_2\vec{a}_2$$

Advanced Materials 35, 2370273 (2023)

Faraday Discussions 173, 137 (2014); Ann der Phys 527, 359 (2015)

‘String theory’ for tuneable domain wall networks: comparison with STM data taken on WS_2 bilayers

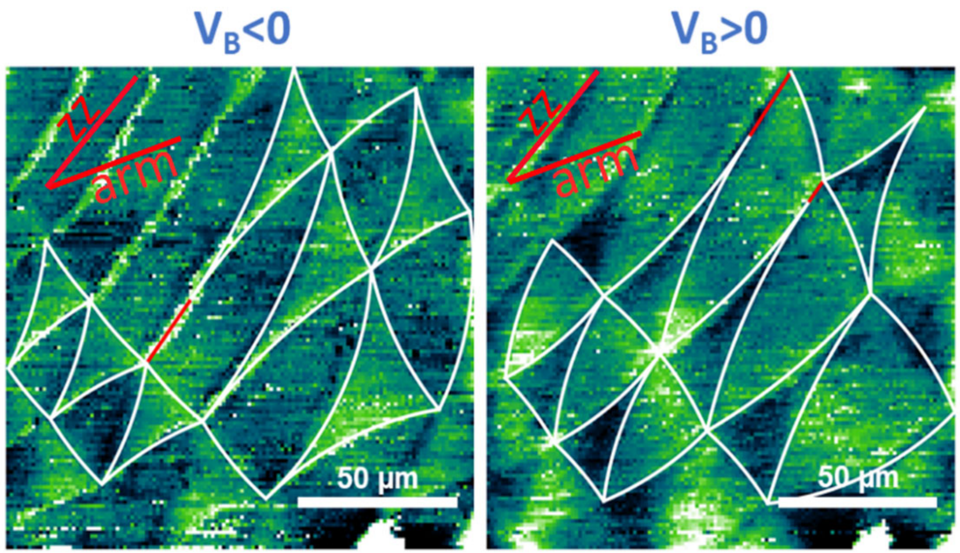

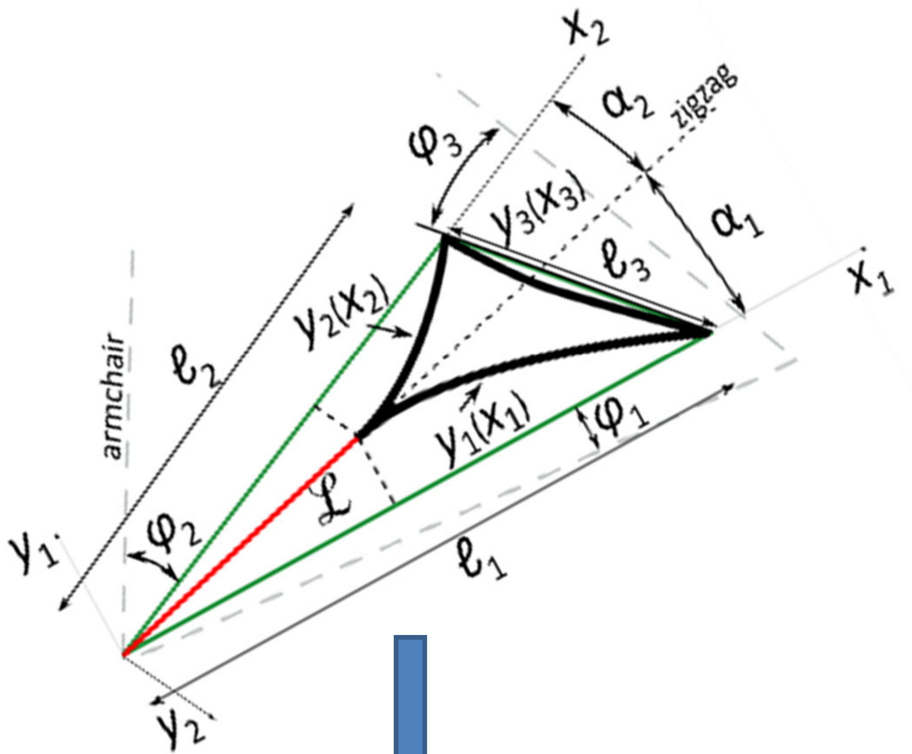

‘string theory’ generalised for anisotropically shaped domains.

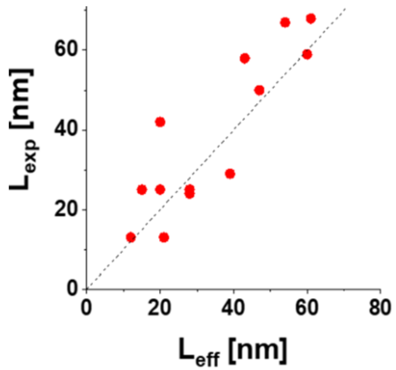

Advanced Materials 35, 2370273 (2023)

Polarisation and hysteresis in the FE tunnelling transistor

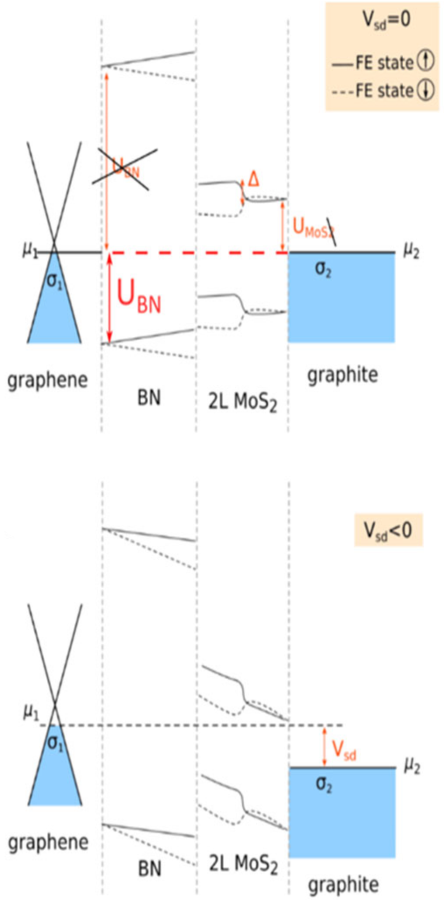

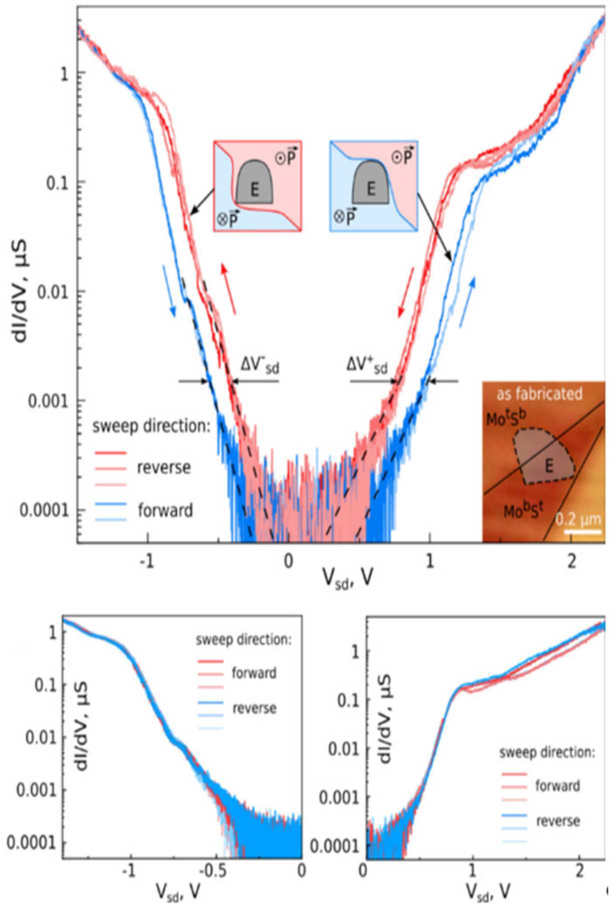

$$ln \frac{dI}{dV_{sd}}\bigg|_{V_{sd}>0} \propto |eV_{sd}| \pm \frac{\delta_>}{2}, \qquad \delta_> \approx \frac{2\sigma(1+\theta)}{2+\sigma+\theta}\Delta$$

$$ln \frac{dI}{dV_{sd}}\bigg|_{V_{sd}<0} \propto |eV_{sd}| \pm \frac{\delta_<}{2}, \qquad \delta_< \approx \frac{2\sigma(1+\theta)}{2\theta\sigma+\sigma+\theta}\Delta$$

$$\sigma = \frac{d_{BN}}{d_{MoS}}\frac{\epsilon_{MoS}}{\epsilon_{BN}}, \theta = \frac{d_{MoS}}{d_{BN}}\sqrt{\frac{m_{MoS}U_{BN}^3}{m_{BN}U_{MoS}^3}}$$

NGI team, unpublished (2023)

Layer-asymmetric band edge states in optics
opposite linear Stark shifts for excitons in MX' and XM' stacking domains

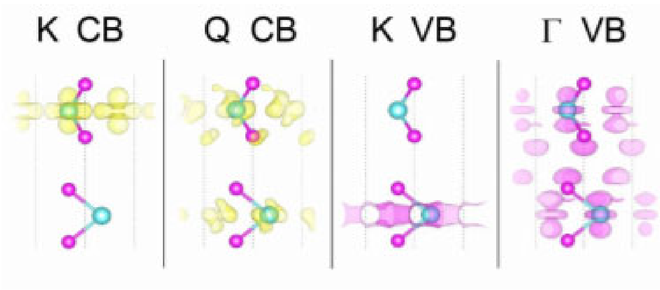

$\|\psi\|^2$ (%)		K CB	Q CB	K VB	Γ VB
Top	Se	3.8	6.5	0.0	1.0
	Mo	92.2	42.6	0.7	31.9
	Se	3.8	10	0.2	14.3
Bottom	Se	0.0	6.8	7.5	14.9
	Mo	0.1	29.7	84.0	36.6
	Se	0.0	4.3	7.5	1.2
d_z (e·nm)		0.322	0.058	-0.317	-0.017

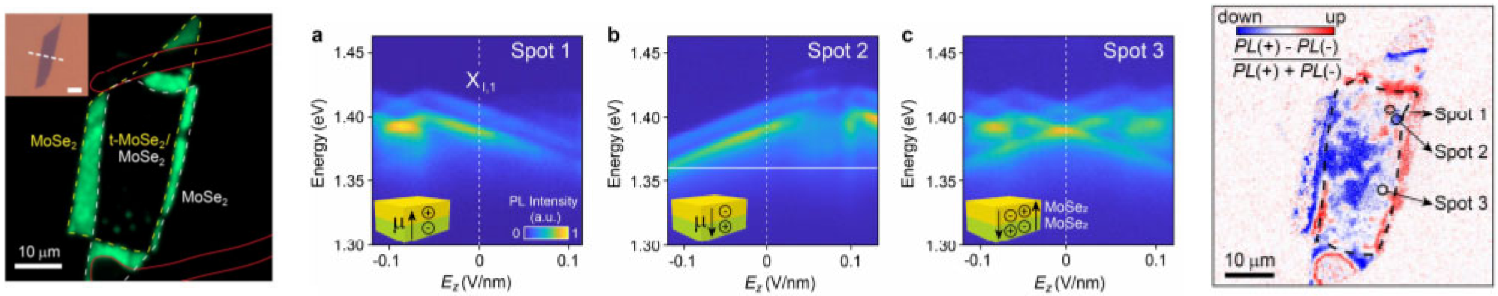

Possible optical read-out of gate-controlled P-bilayer transistor

Nature Nanotechnology 15, 750 (2020)

Layer-asymmetric band edge states in P-MoS_2/ MoS_2 and P-WS_2 /WS_2 : tunnelling characteristics

R-type bilayers lack both mirror reflection and inversion symmetries

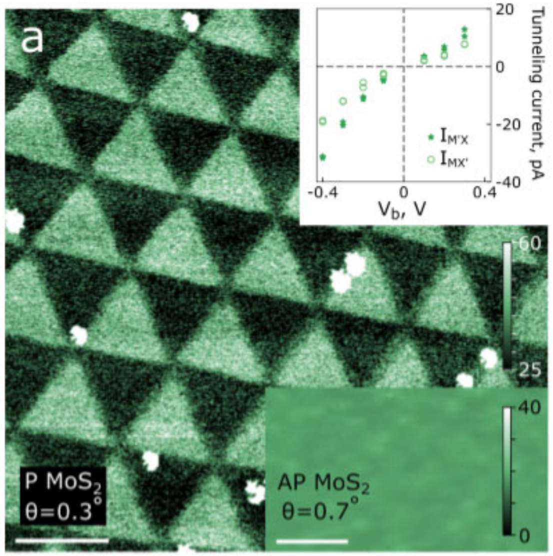

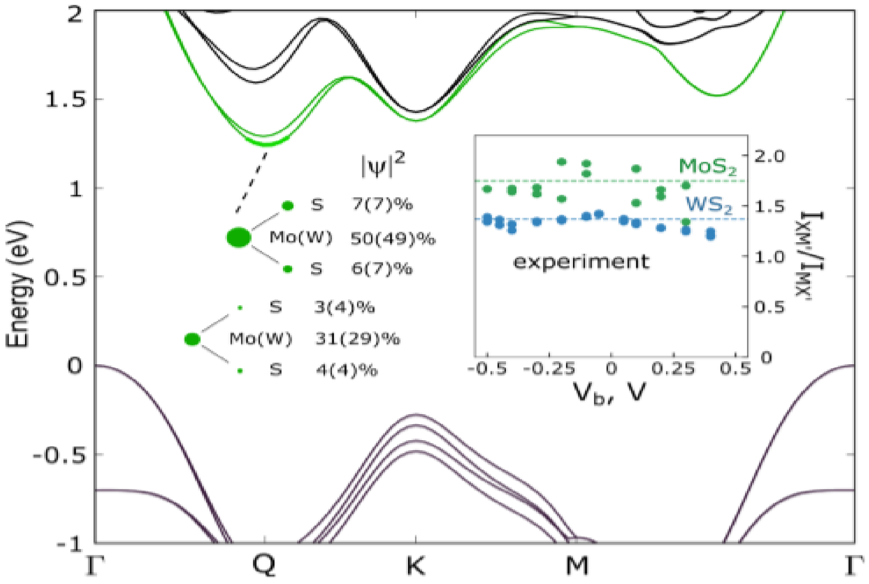

conductive AFM scanning reveals different tunnelling I(V) characteristics for twinned 'R'-type domains (MX' and XM')

weight of electrons' wavefunctions in the bands (Q-valley) differ for the top and bottom layers

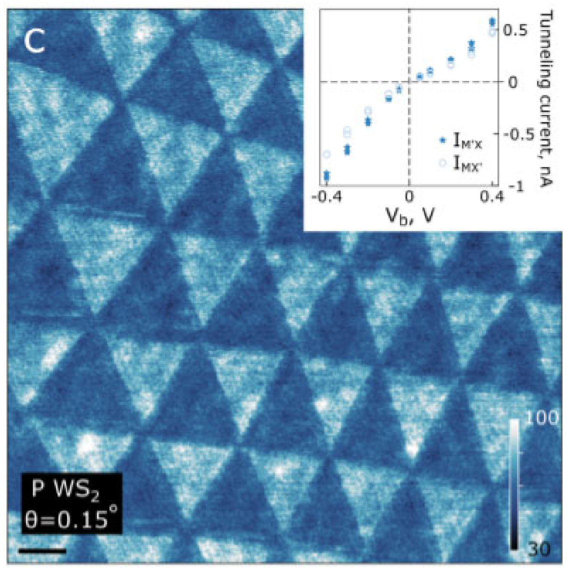

Nature Nanotechnology 15, 592 (2020)

Switching of largest domains: route towards a memristor functionality?

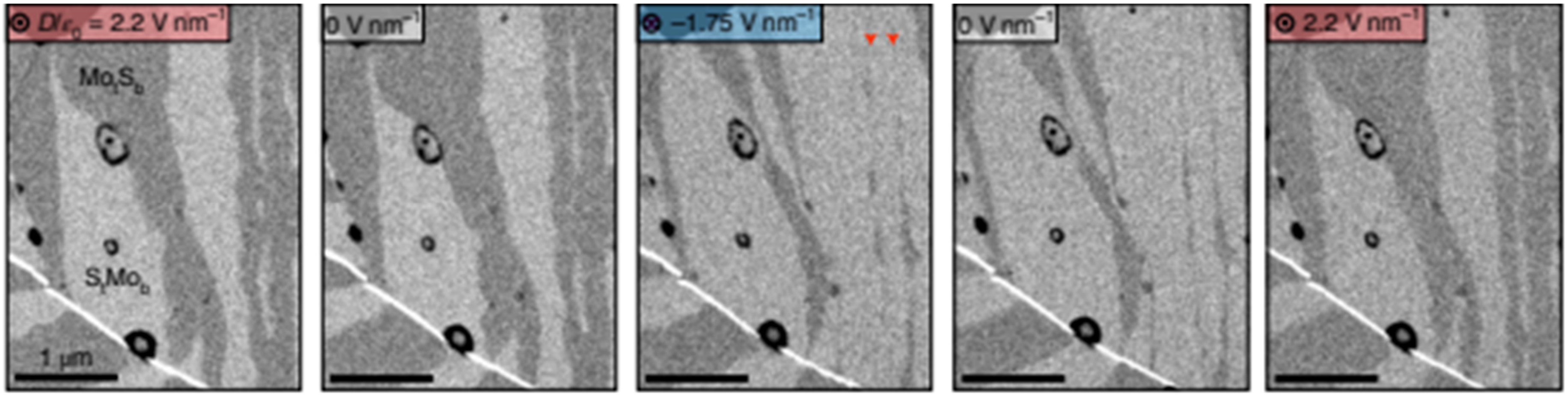

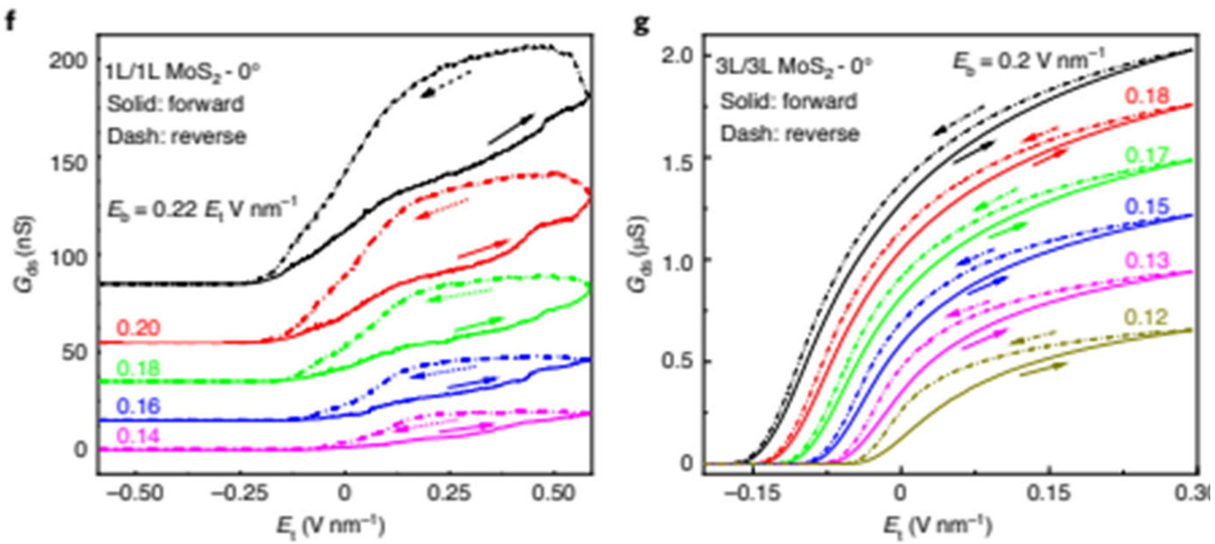

gate-controlled P-bilayer MoS_2 transistor: $G(V_g)$ reflects the FE polarisation of large domain areas

Nature Nanotechnology 17, 390 (2022)

Twistronics of transition metal dichalcogenides

- Structure of twisted bilayers – reconstruction into domains and domain wall networks
- Bilayer with inversion symmetry (AP) and without it (P)
- Ferroelectric interfaces and layer-asymmetric band edges in TMDs
- Switching FE polarisation by sliding and ‘string theory’ for domain wall networks
- Band-edge profiles, arrays of QDs, and ‘narrow moiré minibands’
- Ferroelectric few-layer graphene

QDs and moiré superlattice minibands in small-angle twisted P-homobilayers of MoS_2, $MoSe_2$, WS_2

boxes for Γ-valley holes in 2H domains

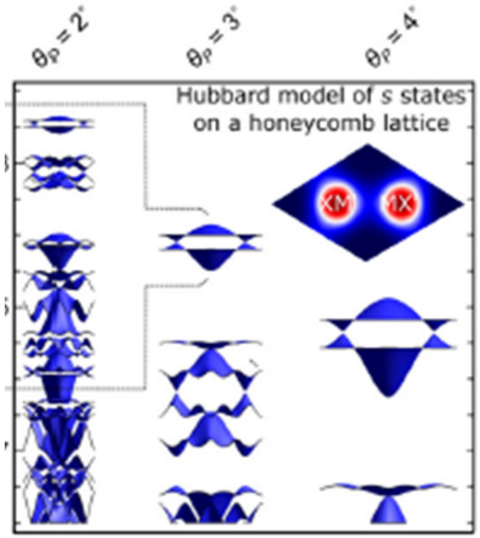

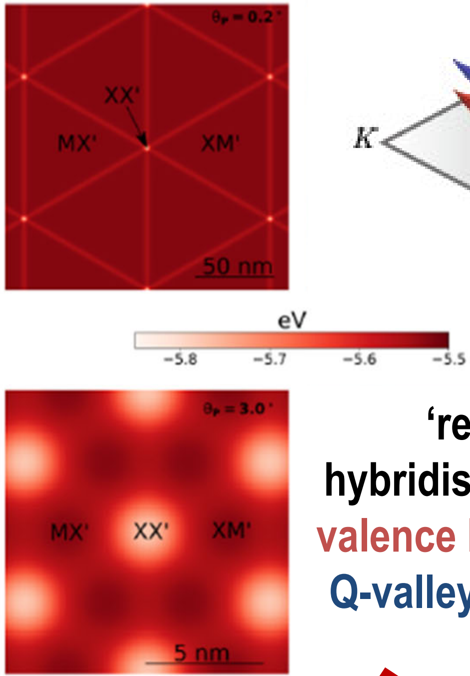

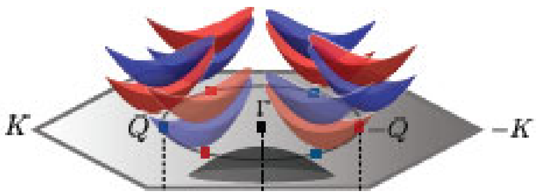

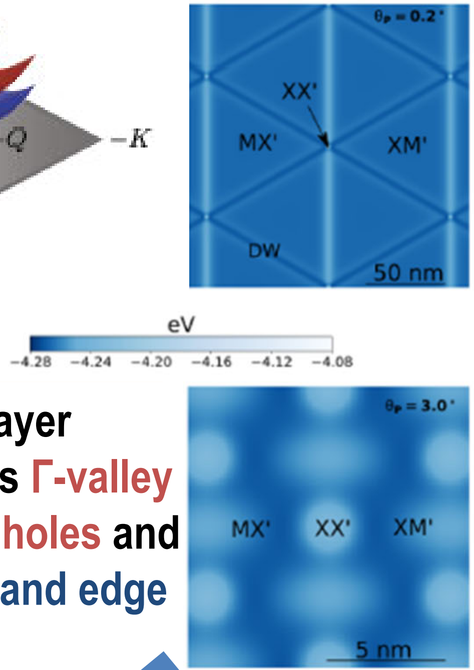

Networks of quantum wires for Q-valley electrons

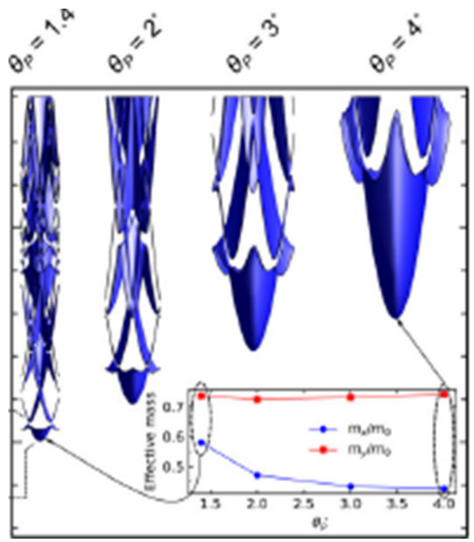

'resonant' interlayer hybridisation promotes Γ-valley valence band edge for holes and Q-valley conduction band edge for electrons

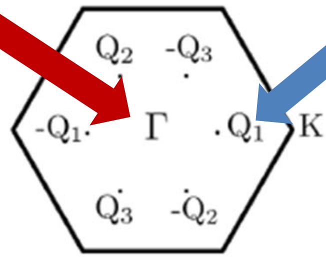

honeycomb pattern with a strong interlayer hybridisation

Appl Phys Lett 118, 241602 (2021)

QDs and moiré superlattice minibands in small-angle twisted AP-homobilayers of MoS_2, $MoSe_2$, WS_2 – for Γ-valley holes and Q-valley electrons

boxes for Γ-valley holes in 2H domains

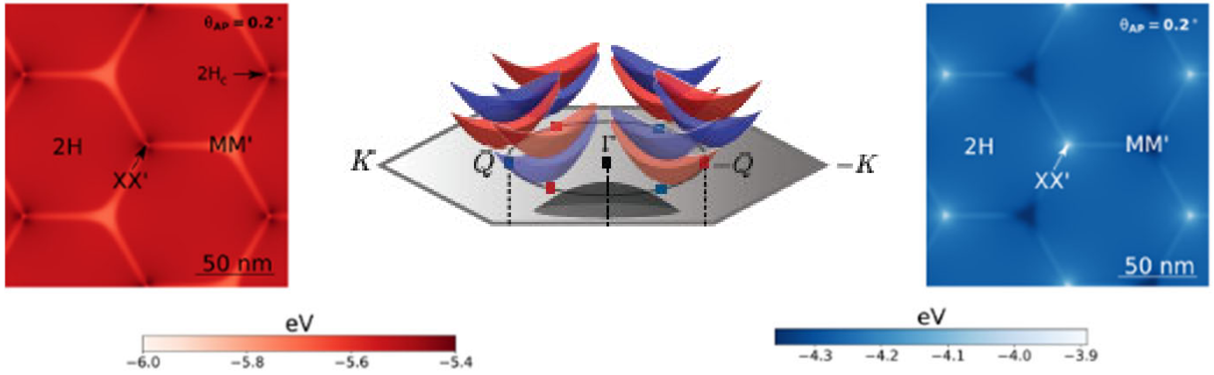

QDs for Q-valley electrons in MM' corners

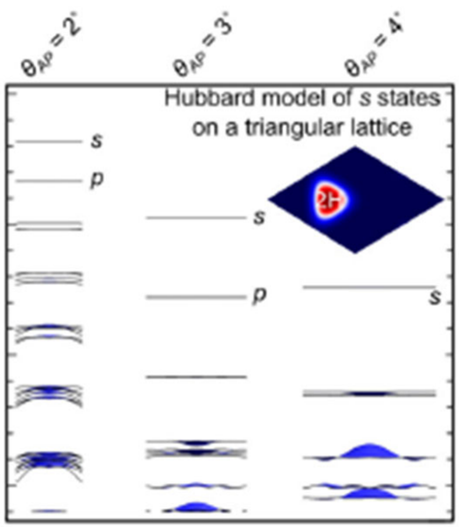

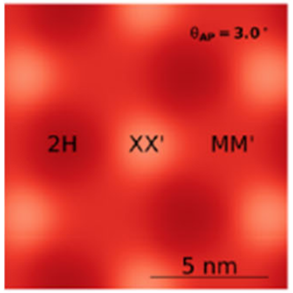

'resonant' interlayer hybridisation promotes Γ-valley valence band edge for holes and Q-valley conduction band edge for electrons

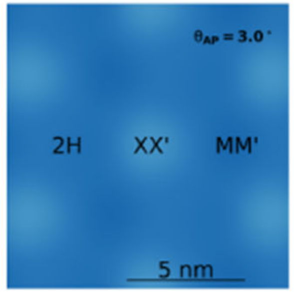

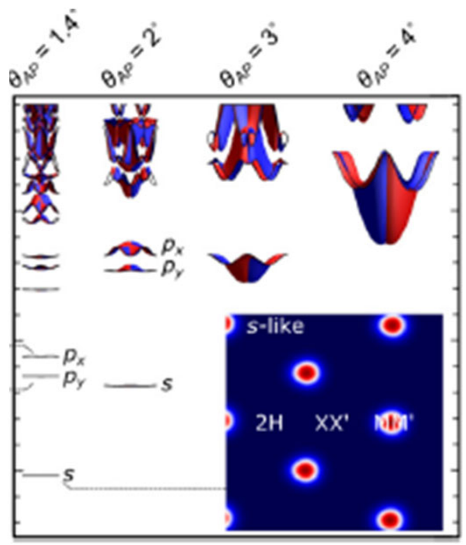

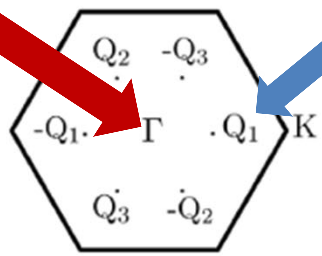

Appl Phys Lett 118, 241602 (2021)

Twistronics of transition metal dichalcogenides

V Enaldiev (NGI / МФТИ)
A Garcia-Ruiz (NGI)
F Ferreira (CDT NOWNANO)
A McEllistrim (CDT NOWNANO)
S Magorrian (NGI / Warwick)
V Zolyomi (NGI / Daresbury Lab)
C Yelgel (NGI / Erdogan Univ)

R Gorbachev (NGI)
S Haigh (NGI)
A Geim (NGI)
O Kazakova (NPL)
P Beton (Nottingham)
A Luican-Mayer (Ottawa)
M Ben Shalom (Tel Aviv)
H Park (Harvard)
P Kim (Harvard)

EPSRC
erc
GRAPHENE NOWNANO CDT
GRAPHENE FLAGSHIP